Impact of nanomechanical resonances on lasing from electrically pumped quantum dot micropillars

T. Czerniuk, J. Tepper, A. V. Akimov, S. Unsleber, C. Schneider, M. Kamp, S. Höfling, D. R. Yakovlev, and M. Bayer

Citation: Applied Physics Letters **106**, 041103 (2015); doi: 10.1063/1.4906611

View online: http://dx.doi.org/10.1063/1.4906611

View Table of Contents: http://scitation.aip.org/content/aip/journal/apl/106/4?ver=pdfcov

Published by the AIP Publishing

Impact of nanomechanical resonances on lasing from electrically pumped quantum dot micropillars

T. Czerniuk,[1,a)] J. Tepper,[1] A. V. Akimov,[2] S. Unsleber,[3] C. Schneider,[3] M. Kamp,[3] S. Höfling,[4] D. R. Yakovlev,[1,5] and M. Bayer[1,5]
[1]*Experimentelle Physik 2, TU Dortmund University, 44227 Dortmund, Germany*
[2]*School of Physics and Astronomy, University of Nottingham, Nottingham NG7 2RD, United Kingdom*
[3]*Technische Physik, Physikalisches Institut and Wilhelm Conrad Röntgen-Center for Complex Material Systems, University of Würzburg, Am Hubland, 97074 Würzburg, Germany*
[4]*School of Physics and Astronomy, University of St Andrews, KY16 0SS St Andrews, United Kingdom*
[5]*Ioffe Physical-Technical Institute, Russian Academy of Sciences, 194021 St. Petersburg, Russia*

(Received 3 December 2014; accepted 6 January 2015; published online 26 January 2015)

We use a picosecond acoustics technique to modulate the laser output of electrically pumped GaAs/AlAs micropillar lasers with InGaAs quantum dots. The modulation of the emission wavelength takes place on the frequencies of the nanomechanical extensional and breathing (radial) modes of the micropillars. The amplitude of the modulation for various nanomechanical modes is different for every micropillar which is explained by a various elastic contact between the micropillar walls and polymer environment. © *2015 AIP Publishing LLC*. [http://dx.doi.org/10.1063/1.4906611]

Micrometer-sized pillars obtained by lateral patterning of vertical cavity surface emitting lasers (VCSELs) with quantum dots (QDs) as optically active medium provide an ideal platform for cavity quantum electrodynamical effects.[1–4] Besides this fundamental interest, such micropillar structures are prospective devices as emitters of single or entangled photons for quantum information technology if electrically pumped.[5,6] Recently, it was demonstrated that the nanomechanical properties of VCSELs may be exploited for ultrafast modulation of the laser output of VCSELs.[7,8] These experiments were performed on optically pumped planar VCSELs. For applications, electrical pumping is essential, for which the VCSELs have to be patterned laterally for electrical injection. This patterning changes also their nanomechanical properties which vice versa may be even tailored by the structuring. Exploiting nanomechanical effects in *electrically pumped* micropillar VCSELs would be a significant step forward towards applications of cavity opto-nanomechanics.[9]

The mechanical (i.e., acoustic or phononic) properties of passive micropillars and similar nanoobjects (e.g., nanorods) have been studied experimentally and theoretically in a number of works during the last decade.[10–13] The mechanical resonance frequencies for micropillars can be easily calculated using numerical techniques, e.g., finite element simulations. In some cases, like free standing nanorods with the length much bigger than the radius, the eigenfrequencies can be even determined analytically.[11–14] Typical micropillars with radii between 1 and 10 μm possess gigahertz (GHz) fundamental vibrational modes, which are the challenging frequency range for laser applications, such as optical data transmission.[15] The focus of the present work is to understand the impact of such nanomechanical modes on the laser emission from micropillar VCSELs that are electrically pumped.

The electric contacts lead to specific differences in the nanomechanical properties in comparison to free-standing micropillars. These differences arise from the planarization of the structure by a polymer surrounding the pillars and coming thereby in touch with them.[4] Polymer and semiconductor have different acoustic impedances. The contact between them is expected to lead to changes of the nanomechanical properties which govern the modulation of laser emission. The detailed changes depend on the quality of the elastic contact between micropillar and polymer.

In the present work, we study the temporal evolution of the laser emission in a number of electrically pumped VCSELs after the impact of a picosecond strain pulse, which excites nanomechanical micropillar modes. We observe that the excited nanomechanical vibrations modulate the wavelength and intensity of the laser output. The modulation spectrum covers a wide frequency range from 0.1 to 1.2 GHz, while the spectral position of the maximum depends on the particular VCSEL. From analyzing the nanomechanical spectrum of the micropillars numerically, we suggest a qualitative explanation for the experimental observations that is based on the different quality of the elastic contact between micropillar and polymer environment in the different studied VCSELs.

The sample used hosts several arrays of electrically pumped micropillar VCSELs, and a corresponding scanning electron microscopy image of a micropillar cross-section is shown in Fig. 1(a). These micropillars are based on a planar microcavity structure consisting of two distributed Bragg reflectors (DBRs) formed by alternating layers of GaAs and AlAs with layer thicknesses of 68 nm and 77 nm, respectively. The bottom DBR at the (100)-orientated GaAs substrate side consists of 27 double-layers, while the top DBR is made of 23 double layers. A GaAs λ-cavity layer is placed between the bottom and top DBRs. This layer contains a sheet of $Ga_{0.7}In_{0.7}As$ QDs in the center that serve as the optically active medium. In order to electrically inject electron-hole pairs into the QDs, the substrate and the bottom DBR are n-doped, while the top DBR is p-doped. Arrays of micropillars with diameters of $d = 3\,\mu$m and $d = 4\,\mu$m are etched out of this planar structure that is afterwards filled up with

a)Thomas.Czerniuk@tu-dortmund.de

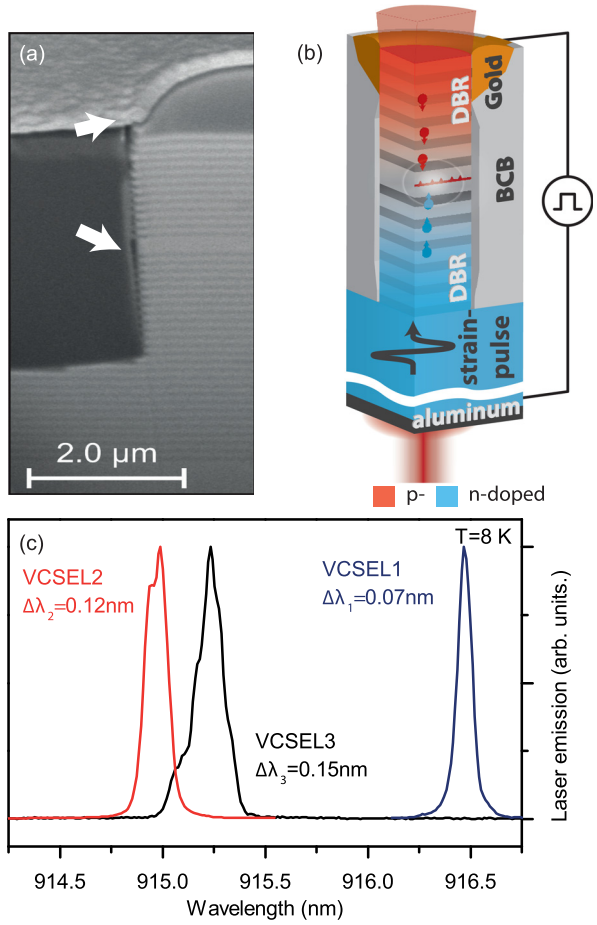

FIG. 1. Experimental arrangements. (a) Scanning electron microscopy image of the micropillar cross-section; the defect interface (marked by white arrows) between the micropillar wall and polymer environment is seen on the image as a light gray strip. (b) Scheme of the experiment with the picosecond strain pulses excited by a femtosecond laser in the Al film deposited on the side of the GaAs substrate opposite to the VCSELs. (c) The laser emission spectra of three studied VCSELs showing different laser line widths.

the polymer benzocyclobutene (BCB). The polymer filling mechanically supports gold rings on top of the micropillars used as the electric contacts to the micropillars. The length of the micropillars is $l = 6.6\,\mu$m. More details about fabrication, electrical and optical characteristics of the used micropillar VCSELs can be found in an earlier publication.[16] A 100 nm thin Al film is deposited on the polished substrate on the backside of the sample, which allows the generation of the acoustic pulse and serves as the second electric contact as well.

Figure 1(b) shows the scheme of the experiment. The picosecond strain pulses with an amplitude of $\sim 10^{-3}$ are excited by femtosecond laser pulses hitting the Al film.[17] The pulses propagate with the sound velocity through the GaAs substrate and hit the micropillars about $t_0 \approx 19$ ns after their generation, thereby coherently exciting resonant elastic (nanomechanical) modes in the pillars. In the experiment, we study the temporal/spectral evolution of the laser output in the 12.5 ns time interval after the impact of the picosecond strain pulse at t_0. For this purpose, we use a spectrometer and a streak camera with spectral and temporal resolutions of 0.05 nm and 50 ps, respectively.

The experiment is carried out at a cryogenic temperature of $T = 8$ K. Under electrical excitation, a VCSEL emits laser light with a central wavelength λ_0 that is determined by the photonic resonance of the structure. For the experiment, we selected different micropillar VCSELs which show a similar laser threshold bias. Emission spectra for three different VCSELs electrically driven well above the laser threshold are shown in Fig. 1(c). VCSEL1 shows the smallest laser linewidth with a full width at half maximum (FWHM) of $\Delta\lambda_1 = 0.07$ nm. The two other VCSELs demonstrate a much broader emissions with $\Delta\lambda_2 = 0.12$ nm and $\Delta\lambda_3 = 0.15$ nm for VCSEL2 and VCSEL3, respectively.

All VCSELs show a modulation of the laser emission $I(t,\lambda)$ as result of the picosecond strain pulse impact, but the modulation amplitude and frequency depend strongly on the particular VCSEL. In the following, we will concentrate on the results obtained for three VCSELs which spectra are shown in Fig. 1(c). Streak camera images of the measured $I(t,\lambda)$ are shown in the left panels of Fig. 2 and correspond to VCSELs 1 and 3 with $d = 3\,\mu$m and VCSEL 2 with $d = 4\,\mu$m. The temporal evolutions of the central wavelength $\lambda_c(t)$ of the laser emission are shown in the streak camera images by the solid black lines and the right panels in Fig. 2 show the fast Fourier transforms (FFT) of $\lambda_c(t)$.

It is seen from Fig. 2 that the laser output of all VCSELs undergoes oscillations of λ_c, but the spectra of these oscillations are very different. Indeed, for VCSEL1 the spectrum of the oscillations of $\lambda_c(t)$ [right panel in Fig. 2(a)] shows three lines with maxima at $f_0 = 0.18$ GHz, $f_1 = 0.47$ GHz, and

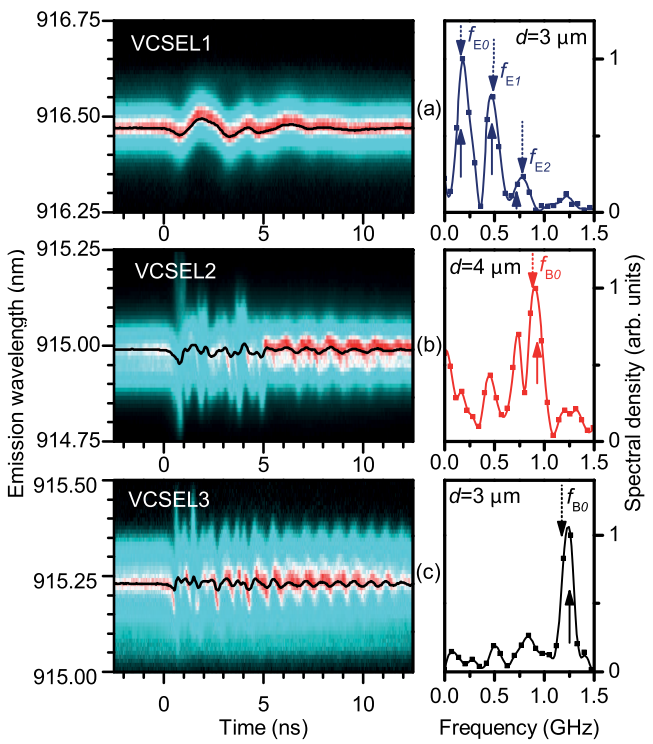

FIG. 2. Laser wavelength modulation. Streak camera images (left panels) of the laser emission of the three studied VCSELs. Red color corresponds to maximum intensity, and the evolution of the central emission wavelength $\lambda_c(t)$ is shown by solid black lines. Right panels show fast Fourier transforms $\lambda_c(t)$ for $\lambda_c(t)$. Vertical arrows in right panels indicate the numerically (solid arrows) and analytically (dashed arrows) calculated frequencies of the extensional (E) and breathing (B) modes.

$f_2 = 0.77$ GHz from which the maximum at f_0 is the dominant one. The VCSEL2 and VCSEL3 spectra [Figs. 2(b) and 2(c), respectively] show maxima at $f = 0.90$ GHz and 1.24 GHz, respectively. This high-frequency line is to a good approximation the only one for the micropillar with $d = 3\,\mu$m [Fig. 2(c)] so that in this case the oscillation of $\lambda_c(t)$ for VCSEL3 can be considered as single harmonic with a quality factor $\sim$10.

The temporal evolution of the spectrally integrated intensity $I(t)$ of the laser emission also shows oscillations as demonstrated in Fig. 3(a). These oscillations are weak in VCSEL1 but reach 40% in VCSEL2. The FFT of $I(t)$ from VCSEL2 and VCSEL3 shown in Fig. 3(b) exhibit single spectral lines with maxima at the frequencies $f = 0.90$ GHz and 1.24 GHz, respectively, exactly as in the FFT of $\lambda_c(t)$ in Figs. 2(b) and 2(c).

For understanding the experimental results, we consider the nanomechanical properties of micropillar VCSELs. The picosecond strain pulse arriving at the VCSEL array from the backside of the sample excites coherent vibrations that result in a dynamical atom displacement accompanied by mechanical strain in the micropillars. The displacement along the z-direction (i.e., parallel to the micropillar axis) modulates the thickness of the layers while dynamical strain tensor components ε_{ij} may affect the dielectric permittivity tensor in the DBRs and the laser cavity.[18] Both effects can result in a modulation of the VCSELs output $I(t,\lambda)$. The first step in our analysis is to calculate the frequencies of the localized nanomechanical eigenmodes in the studied micropillars and compare them with the values measured experimentally. The eigenfrequency calculation for a VCSEL with length l and diameter d is performed by using the finite element method, taking into account the GaAs substrate but omitting the polymer which surrounds the micropillar. The results of the calculations are shown in the right panels of Fig. 2 by the vertical solid arrows. These numerically calculated values are close to the values obtained analytically for the extensional (E) and breathing (B) vibrational modes of a cylinder with $l \gg d/2$ (for the extensional modes one end of the cylinder is assumed to be fixed). The E- and B-modes have very different characteristics for the displacement and strain distributions in the micropillars: E-modes correspond to localized longitudinal vibrations along the z-direction; B-modes are radial modes for which the strain tensor component $\varepsilon_{zz} = 0$. The analytical expressions for the frequencies f_{En} and f_{Bn} of the nth E- and B-mode are[11–14]

$$f_{En} = \frac{2n+1}{4l}\sqrt{\frac{Y}{\rho}}; \quad f_{Bn} = \frac{\tau_n s}{\pi d}, \tag{1}$$

where Y is Young's modulus along the axis of the micropillar, ρ is the density, s is the longitudinal sound velocity, and $\tau_n \sim 1$ is a dimensionless parameter determined by a transcendental algebraic equation, see Ref. 12. For all material parameters, we used the mean values of GaAs and AlAs weighted by their content within the micropillar: $Y = 84.34$ GPa, $s = 5219$ m/s, and $\rho = 4.50$ g/cm^3.

The dashed vertical arrows in the right panels of Fig. 2 show the values for f_{E0}, f_{E1}, f_{E2}, and f_{B0} calculated using Eq. (1). Since the analytical and numerical calculations (compare the positions of the solid and dashed arrows) give similar values for the vibrational frequencies, we can identify whether a numerically calculated frequency corresponds to an E- or a B-mode. The validity of this classification has also been confirmed by varying micropillar height l and diameter d in the calculations. The numerically calculated values of f_{En} and f_{Bn} show a linear dependence on l^{-1} and d^{-1}, respectively, which is in full agreement with the analytical expression in Eq. (1).

Furthermore, the right panels of Fig. 2 show good agreement between the experimental and calculated values of the mode frequencies. For instance, the calculated values of f_{E0}, f_{E1}, and f_{E2} marked by arrows fit well the measured spectral positions of the maxima in VCSEL1. The calculated values of f_{B0} match the maxima of the measured spectral lines in VCSEL2 and VCSEL3 with $d = 4$ and $3\,\mu$m, respectively. This agreement validates the appropriateness of our theoretical approach and allows us to attribute the experimentally measured spectral lines in the different micropillars to the E- or B-modes.

The main result of the experiment and the corresponding analysis is that the resonant nanomechanical vibrations at the frequencies of the E- and B-modes distinctly appear in the modulation of the central wavelength of the laser output. However, the question that obviously arises from the set of experimental data is why in different VCSELs, even with nominally identical geometries, maximum modulation amplitude occurs at different nanomechanical modes with respect to character and frequency: VCSEL1 does not show a distinct B-mode as can be seen in Fig. 2(a); the FFT of $\lambda_c(t)$ in Fig. 2(b) for VCSEL2, on the other hand, exhibits well defined spectral lines for both E- and B-modes; and in VCSEL3 the B-mode strongly dominates the FFT spectrum in Fig. 2(c).

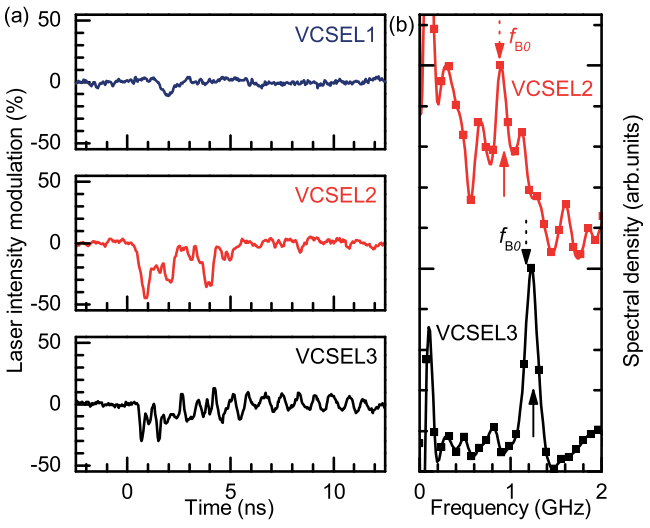

FIG. 3. Intensity modulation. (a) The temporal evolutions of the laser output modulation of the intensity $I(t)$ integrated over the spectral range, obtained from the streak camera images (left panels of Fig. 2) for the three VCSELs. (b) Fast Fourier transforms of $I(t)$ for VCSEL2 and VCSEL3, which show the spectral peak at the frequency of the nanomechanical B-mode. The vertical arrows show the numerically (solid arrows) and analytically (dashed arrows) calculated frequency f_{B0} for the B-mode.

To explain the difference of the modulation spectra in the different VCSELs, we discuss on a qualitative level the efficiency of the excitation of E and B-modes by a picosecond strain pulse incident from the substrate side. A purely compressive (longitudinal) elastic wavepacket, which propagates through bulk GaAs, is transformed at the interface into a number of bulk and surface modes due to the diffraction at the micropillar edges.[19] The amplitudes of the E- and B-modes are strongly influenced by the elastic contact between the GaAs-based micropillars and the surrounding BCB polymer. This contact may vary strongly between different VCSELs, because the process of etching the micropillars out of the initially planar structure results in pillar sidewalls of different quality and also the polymer planarization may show different quality. In the case of perfect elastic contact, E-modes are easily excited in the micropillars by a strain pulse propagating in the BCB film in z-direction, but B-modes are difficult to launch due to the micropillar walls being covered by the BCB, despite of some acoustic impedance mismatch between the materials. Applying this qualitative model to the experimental results, we may attribute the case of perfect elastic contact to VCSEL1, where only E-modes are observed in the spectrum in Fig. 2(a). Alternatively, in the case of a loose elastic contact with the BCB, B-modes excited at the basis of the micropillars may become the dominant ones in the spectrum, because they are then not expected to leak into the BCB and therefore should have a long lifetime in the micropillars. This extreme case may be attributed to VCSEL3 where only the B-mode is detected [see Fig. 2(c)]. VCSEL2, which shows both E- and B-modes [see Fig. 2(b)], may be attributed to the intermediate case between perfect and loose elastic contact of the micropillar and the BCB environment.

It is interesting that the amplitude of the B-mode in the spectrum of the laser output modulation increases as the emission becomes broader [compare the optical and modulation spectra in Figs. 1(c) and 2]. Based on our results for several VCSELs, it is difficult to say whether this observation is incidental or regular. If the latter is true, the elastic contact with the BCB and the laser linewidth may be related via the micropillar cavity Q-factor: an inhomogeneous micropillar environment may lower the symmetry of the resonator and lead to optical loss channels due to the polymer/air interfaces at the micropillar sidewalls (see Fig. 1(a)). Moreover, a loose elastic contact may be accompanied by an inefficient heat sink and correspondingly a low Q-factor when the VCSEL is electrically pumped.

Finally, we discuss the effects of the nanomechanical resonances on the modulation of the laser intensity output $I(t)$ as demonstrated in Fig. 3. It was shown earlier that dynamical strain can modulate the output intensity in optically excited QD lasers.[7] The effect is strong only for high modulation frequencies f when $f \geq \tau_s^{-1}$, where $\tau_s \sim 1$ ns is the spontaneous lifetime of an electron-hole pair in a QD. In agreement with this statement, we observe a strong modulation of the intensity only by the B-modes with a frequency of $f \sim 1$ GHz in VCSEL2 and VCSEL3 while the low frequency E-modes do not induce a notable modulation of $I(t)$.

In conclusion, we have shown that electrically pumped micropillar VCSELs affected by a picosecond strain pulse show GHz oscillations of the laser output. The modulation spectrum is well described by the extensional (E) and the breathing (B) nanomechanical modes of the micropillars. Which modes contribute to the laser output modulation depends on the particular VCSEL: we explain the difference in the modulation spectra of the studied VCSELs by the variation of the elastic contact between the micropillar and the surrounding polymer.

The potential applications of nanomechanical resonances in micropillar VCSELs go far beyond sole modulation of the laser emission, which may be achieved also by other established techniques.[15,20] Exploitation of opto-nanomechanical and cavity quantum electrodynamical effects in quantum information technologies is widely discussed nowadays. Our work demonstrates that the impact of nanomechanical resonances in electrically pumped VCSELs is much stronger than in passive optomechanical devices. Electrical pumping of VCSELs provides a step forward towards usage of optomechanical properties in a single compact chip with integrated nanophotonic and phononic circuits without external optical sources. For the excitation of phonon resonance at GHz frequencies, it is realistic nowadays to use short electrical pulses applied to the VCSEL. The efficiency of electrical excitation can be enhanced in micropillars grown on substrates along a piezoelectric active orientation. Achieving a breakthrough in high-frequency (10^{11}–10^{12} Hz) nanomechanics with electrically pumped VCSELs will be to excite nanomechanical resonances in the way how it is done in passive superlattices[21] and phonon microcavities with optical DBRs.[22]

We acknowledge Boris Glavin for fruitful discussions. The work was sponsored by the German Ministry of Education and Research (BMBF) within the RELQUSA project (FKZ: 13N12462) and the Deutsche Forschungsgemeinschaft (Ba1549/14-1 and Collaborative Research Centre TRR 142). The work was also supported by the state of Bavaria. A.V.A. acknowledges the Alexander-von-Humboldt Foundation. S.H. acknowledges support by the Royal Society and the Wolfson Foundation.

[1]K. J. Vahala, Nature **424**, 839 (2003).
[2]S. Strauf, N. G. Stoltz, M. T. Rakher, L. A. Coldren, P. M. Petroff, and D. Bouwmeester, Nat. Photonics **1**, 704 (2007).
[3]G. Khitrova, H. M. Gibbs, M. Kira, S. W. Koch, and A. Scherer, Nat. Phys. **2**, 81 (2006).
[4]C. Schneider, A. Rahimi-Iman, N. Y. Kim, J. Fischer, I. G. Savenko, M. Amthor, M. Lermer, A. Wolf, L. Worschech, and V. D. Kulakovskii, Nature **497**, 348 (2013).
[5]P. Michler, A. Kiraz, C. Becher, W. V. Schoenfeld, P. M. Petro, L. Zhang, E. Hu, and A. Imamoglu, Science **290**, 2282 (2000).
[6]A. Dousse, J. Suffczynski, A. Beveratos, O. Krebs, A. Lemaıtre, I. Sagnes, J. Bloch, P. Voisin, and P. Senellart, Nature **466**, 217 (2010).
[7]C. Brüggemann, A. V. Akimov, A. V. Scherbakov, M. Bombeck, C. Schneider, S. Höfling, A. Forchel, D. R. Yakovlev, and M. Bayer, Nat. Photonics **6**, 30 (2012).
[8]T. Czerniuk, C. Brüggemann, J. Tepper, S. Brodbeck, C. Schneider, M. Kamp, S. Höfling, B. A. Glavin, D. R. Yakovlev, A. V. Akimov, and M. Bayer, Nat. Commun. **5**, 4038 (2014).
[9]M. Aspelmeyer, T. J. Kippenberg, and F. Marquardt, "Cavity optomechanics," Rev. Mod. Phys. **86**, 1391 (2014).
[10]H. Sakuma, M. Tomoda, P. H. Otsuka, O. Matsuda, O. B. Wright, T. Fukui, K. Tomioka, and I. A. Veres, Appl. Phys. Lett. **100**, 131902 (2012).
[11]G. V. Hartland, M. Hu, O. Wilson, P. Mulvaney, and J. E. Sader, J. Phys. Chem. B **106**, 743 (2002).

[12]M. Hu, X. Wang, G. V. Hartland, P. Mulvaney, J. P. Juste, and J. E. Sader, J. Am. Chem. Soc. **125**, 14925 (2003).
[13]P. A. Mante, H. P. Chen, Y. C. Wu, C. Y. Ho, L. W. Tu, J. K. Sheu, and C. K. Sun, AIP Conf. Proc. **1506**, 2 (2012).
[14]L. D. Landau, E. M. Lifshitz, A. M. Kosevich, and L. P. Pitaevskii, *Theory of Elasticity* (Butterworth-Heinemann, 1986).
[15]W. Hofmann, M. Müller, P. Wolf, A. Mutig, T. Gründl, G. Böhm, D. Bimberg, and M.-C. Amann, Electron. Lett. **47**(4), 270 (2011).
[16]S. Reitzenstein, T. Heindel, C. Kistner, A. Rahimi-Iman, C. Schneider, S. Höfling, and A. Forchel, Appl. Phys. Lett. **93**, 061104 (2008).
[17]C. Thomsen, H. T. Grahn, H. J. Maris, and J. Tauc, Phys. Rev. B **34**, 4129 (1986).
[18]T. Berstermann, C. Brüggemann, M. Bombeck, A. V. Akimov, D. R. Yakovlev, C. Kruse, D. Hommel, and M. Bayer, Phys. Rev. B **81**, 085316 (2010).
[19]C. Brüggemann, A. V. Akimov, B. A. Glavin, V. I. Belotelov, I. A. Akimov, J. Jäger, S. Kasture, A. V. Gopal, A. S. Vengurlekar, and D. R. Yakovlev, Phys. Rev. B **86**, 121401 (2012).
[20]A. G. Deryagin, D. V. Kuksenkov, V. I. Kuchinskii, E. L. Portnoi, and I. Y. Khrushchev, Electron. Lett. **30**, 309 (1994).
[21]A. Bartels, T. Dekorsy, H. Kurz, and K. Köhler, Phys. Rev. Lett. **82**, 1044 (1999).
[22]A. Fainstein, N. D. Lanzillotti-Kimura, B. Jusserand, and B. Perrin, Phys. Rev. Lett. **110**, 037403 (2013).